Independent yields of the isomers of ^{133}Xe and ^{135}Xe for neutron-induced fission of ^{233}U, ^{235}U, ^{238}U, ^{239}Pu, and ^{242}Am^{m}

G. P. Ford, K. Wolfsberg, and B. R. Erdal
Los Alamos National Laboratory, Los Alamos, New Mexico 87545
(Received 8 March 1984)

Fractional independent yields of ^{133}Xe^{m}, ^{133}Xe^{g}, ^{135}Xe^{m}, and ^{135}Xe^{g} have been measured for fission of ^{233}U, ^{235}U, ^{239}Pu, and ^{242}Am^{m} induced by thermal neutrons and for fission of ^{235}U, ^{238}U, and ^{239}Pu induced by 14-MeV neutrons. The same yields have been measured for fission of ^{235}U induced by degraded fission spectrum neutrons from a bare critical assembly. Some upper limits and ratios of yields of these same isomers have been obtained for the fission of ^{238}U and ^{239}Pu by the degraded fission spectrum neutrons. The average angular momentum of these independently formed fission products has been derived from the measured isomer ratios. A method that is particularly well adapted to use with computers for solving the differential equations of radioactive decay and growth is described.

I. INTRODUCTION

One of the methods used to study the distribution of nuclear charge in fission is to measure the primary or independent yields of individual fission products with radiochemical techniques.[1] Although there have been many such measurements for low-energy neutron-induced fission, the distribution of charge is not as well known as the distribution of mass. The distribution of mass is easier to measure than the distribution of charge because it does not change (except for delayed neutron emission) with time. The primary or independent yields are usually expressed as fractions of the mass-chain yield and called fractional independent yields.

We have measured the fractional independent yields of ^{133}Xe^{m}, ^{133}Xe^{g}, ^{135}Xe^{m}, and ^{135}Xe^{g} for fission of ^{233}U, ^{235}U, ^{239}Pu, and ^{242}Am^{m} induced by thermal neutrons and for fission of ^{235}U, ^{238}U, and ^{239}Pu induced by neutrons with energy near 14 MeV. For fission induced by degraded fission spectrum neutrons, we have measured the same yields for ^{235}U, and we have obtained some upper limits and ratios of yields for ^{238}U and ^{239}Pu. It has been suggested that the independent yields of different spin isomers may provide information about the distribution of angular momentum in fission.[2] The independent yield of ^{135}Xe^{g} is of importance to reactor operation because it has a high capture cross section for thermal neutrons.

For each measurement of Xe fractional independent yields, we did a carefully timed chemical separation (by the emanation method[3]) of Xe from its precursors soon after a neutron irradiation of the fissile target. Another such separation was done after substantial beta decay of the precursors of Xe. The amount of radioactive Xe in each sample was measured by counting the gamma rays with solid state detectors. The emanation method is very suitable for the separation of Xe from its precursors because it is quick and sufficiently complete. Fast separations and short irradiations are needed to minimize corrections for beta decay. If the irradiation were instantaneous and the first Xe separation were immediate, then the first Xe separated would be the directly formed Xe, and the sum of the amounts of Xe from the first and second separations would be a measure of the chain yield. A rapid first separation of Xe is particularly important when the fractional independent yield of Xe is small; otherwise, a large fraction of the measured Xe would result from the decay of precursors.

The irradiations, fissionable materials, and chemical apparatus and manipulations are described. The method of calculating fractional independent yields from the data is described, and the results are presented and discussed. An attempt is made to relate the ratio of the yields of the isomers to the average of the total angular momentum quantum number and average excitation energy of ^{131}Te, ^{133}Te, ^{133}Xe, and ^{135}Xe, but no attempt is made to trace this process back through the various stages of neutron emission to the scission configuration.

II. EXPERIMENTAL METHODS

A. Irradiations

Each result is the average of at least two different irradiations. Most of the irradiations with thermal neutrons were done in the rabbit port of the Los Alamos "Water Boiler" Reactor (now decommissioned). In this position, the flux was $\cong 5\times 10^{11}$ n cm^{-2} sec^{-1}. The ratio of the number of fissions induced by thermal neutrons to the number induced by more energetic neutrons was determined to be 16.9 in this position. This ratio was obtained by measuring the ^{99}Mo activity from ^{235}U irradiated with and without a 0.76-mm cadmium wrapping. The ratio of the independent yields (which we call the isomer ratio) of the isomers of ^{133}Xe and ^{135}Xe for thermal-neutron-induced fission of ^{239}Pu was measured for an irradiation in port TCR-3 (where the cadmium ratio is $\cong 60$ and the flux is $\simeq 5\times 10^{12}$ n cm^{-2} sec^{-1}) of the Los Alamos Omega West Reactor. In this port, the ratio of the number of fissions induced by thermal neutrons to the number induced by more energetic neutrons was determined as

TABLE I. Composition of uranium fissionable materials.

Isotope	^{233}U	^{235}U				^{238}U
	A	*B*	*C*	*D*	*E*	*F*
^{233}U	98.03				0.02	
^{234}U	0.276	1.12	0.065	1.07	1.10	
^{235}U	0.0174	94.13	99.727	93.13	93.09	0.0006
^{236}U			0.080	0.71	0.16	
^{238}U	1.68	4.75	0.128	5.01	5.63	99.999

above to be 465.6. The independent-yield isomer ratios for port TCR-3 agreed within experimental error with those measured for irradiations of ^{239}Pu in the Water Boiler and indicate that the larger fraction of epithermal neutrons of the Water Boiler did not affect the independent-yield isomer ratios.

The irradiations with degraded-fission-spectrum neutrons were done at Godiva-IV.[4] Godiva-IV is a ^{235}U fast-burst, bare critical assembly. It is a cylinder 153 mm high with a radius of 89 mm. Samples were irradiated in a position with their center near the midplane and $\cong 127$ mm from the axis. For one burst, the time-integrated flux was 4×10^{13} n cm^{-2} for a temperature rise of 173 °C. In general, the time-integrated flux is proportional to the temperature rise, which can routinely be as high as 200 °C. The neutron spectrum in this position was characterized by measuring the activity of $^{115}Cd^{g}$ and ^{99}Mo for fission of ^{235}U and comparing these activities with the same activities for thermal-neutron-induced fission of ^{235}U. In this position, $^{115}Cd^{g}$ had 3.07 ± 0.17 times the fission yield for thermal neutrons. Within experimental error, the yield of $^{115}Cd^{g}$ was the same when the ^{235}U was enclosed in 0.76-mm Cd foil. We did not enclose the fissionable material in Cd for any of the fractional independent-yield measurements.

If the two-mode-of-fission hypothesis[5] holds, as it seems to unless thermal-neutron-induced fission of ^{235}U is involved,[6,7] the effect of the Godiva-IV spectrum on fission product yields can be determined by the measurement of two fission products, such as $^{115}Cd^{g}$ and ^{99}Mo. The two-mode-of-fission hypothesis also implies that there is a single-neutron energy that would produce the same fission yields from ^{235}U as are produced by the Godiva-IV spectrum. From the $^{115}Cd^{g}$ fission yields and the measured variation in valley yields with excitation energy,[7,8] we deduce that this energy is between 1.8 and 2.1 MeV.

Some neutron irradiations were done at the Los Alamos Cockroft-Walton Accelerator where the flux was 7×10^{8} n cm^{-2} sec^{-1}, the neutron energy was 14.6 MeV, and the *R* value of $^{115}Cd^{g}$ was 99.4. Other irradiations were done at the Lawrence Livermore National Laboratory Insulated Core Transformer Facility where the flux was 2×10^{11} n cm^{-2} sec^{-1}, the neutron energy was 14.8 MeV, and the $^{115}Cd^{g}$ *R* value was 113 ± 4. These differences were disregarded in averaging the results of different experiments.

B. Composition of fissionable materials

The isotopic composition of all the uranium and plutonium fissionable materials used are given in Tables I and II, respectively. Each material is identified by a letter (*A*, *B*, etc.), which is used to associate fissionable materials with measured yields to be presented. No isotopic analysis is available for the plutonium used for some of the irradiations with 14.8-MeV neutrons. The material is typical Hanford weapons grade plutonium of the 1955–1960 period, and its specific activity is 1.64×10^{8} disintegrations per minute per milligram.[9] The letter *I* is associated with this material. The composition of material *G* in Table II is typical of this type of plutonium. The americium was a portion of the enriched $^{242}Am^{m}$ prepared by Hoff *et al.*[10] Its composition is: ^{242}Cm, 0.17%; ^{241}Am, 79.38%; $^{242}Am^{m}$, 19.75%; and ^{243}Am, 0.70%. Although $^{242}Am^{m}$ is not the major component, it accounts for 99.8% of the fissions because of its very large (7600 b) (Refs. 11 and 12) fission cross section.

C. Chemistry and manipulations

The emanation method was adapted for our measurements as follows. The fissile targets were either powdered stearates or thin foils of oxides on 0.13-mm-thick platinum. The uranium and plutonium deposits were 8 mm by 39 mm and contain from 0.8 to 1.0 mg of fissile material. The americium foil has been described in Ref. 11. When foils of fissile materials were used, either one foil or two foils back to back were placed in either a polycarbonate or aluminum tube 1.0- to 1.8-cm i.d. by 7 to 10 cm long. The foils were covered with $\cong 0.5$ g of praseodymium stearate. The ends of the tubes were plugged with quartz wool and rubber stoppers. When stearates of uranium were used, there was a layer of praseodymium stearate separating the fissile material from the quartz wool. When uranyl stearate was used in a polycarbonate tube, the tube was lined with 0.13-mm-thick platinum. Plutonyl stearate encapsulating cylinders were made of aluminum with stainless steel frits at each end and were 4.42-cm long by 1.58-cm o.d. and contained $\cong 0.5$ g of plutonyl stearate (material *I* above). For irradiation, the capsules of plutonyl stearate were placed inside aluminum tubes with rubber stoppers in the ends and with aluminum spacers to provide a space between the rubber stoppers

TABLE II. Composition of plutonium fissionable materials.

Isotope	*G*	*H*
^{238}Pu		0.002
^{239}Pu	94.41	99.27
^{240}Pu	5.23	0.71
^{241}Pu and ^{241}Am	0.36	0.01
^{242}Pu		<0.001

and the capsule. In all cases, the tubes with rubber stoppers were evacuated through a number 23 hypodermic needle inserted through one of the stoppers. The needle was removed, and the rabbit was irradiated for a short time and then rapidly transported to a suitable place where a number 16 hypodermic needle attached to a vessel containing $\cong$3 mg of inactive xenon was inserted through one of the rubber stoppers. A similar needle, leading to an evacuated tube containing a train of two charcoal traps, each $\cong$2-mm i.d. by 1-cm long, was inserted through the rubber stopper in the other end of the rabbit. The trap farthest from the rabbit was cooled with liquid nitrogen, and the other trap was heated to $\cong$150°C with a hot-air gun. Inactive xenon was admitted to the rabbit by momentarily opening a stopcock. After a few seconds to allow mixing with radioactive xenon, the stopcock to the cold trap was opened and the xenon was condensed. The stopcock to the cold trap was then closed, the stopcock to the inactive xenon vessel was again opened, and the cycle was repeated. The cold trap was sealed off and mounted for counting, and the hypodermic needles were withdrawn. A day later, most of the xenon that had grown in by decay of precursors was removed by the same procedure.

It is known[13] that praseodymium, uranyl, and plutonyl stearate emanate noble gases quantitatively in a fraction of a second in the absence of air (as discussed later), whereas the platinum backing of the fissile foils and the aluminum tubes retain noble gases nearly completely (0.3% emanate in 24 h). For our purposes it is not necessary to know the emanating properties of polycarbonate or quartz wool because no fission fragments were incident on these materials. Emanation from rubber stoppers is discussed later. Our measurements indicate that between 0.04% and 0.4% of the radioactive I and their Te and Sb precursors emanate from the stearates and are removed from the apparatus within the times involved in our experiments. However, $>$99% of this small fraction is retained in the warm charcoal trap. Thus the overall decontamination of xenon from precursors is $>10^4$. For the first Xe separation and for the irradiation containers used in thermal neutron irradiations, our measurements indicate that for condensation times of 2, 1, and 0.5 min, 99%, 97%, and 95%, respectively, of the xenon in the irradiation container condensed in the cold trap. For the first Xe separation and for the containers used in 14-MeV neutron irradiations of uranium, it was found that 99.6% of the xenon condensed in the cold trap. These factors were used in the chemical separation matrix C_1 to be described.

In a series of experiments with times chosen appropriately for measuring cumulative yields, it was found that the ^{133}Xe and ^{135}Xe yields from a second separation at about 1 d were about 16% lower than from a first separation at about 4 h. This effect was the subject of several experiments described below.

In one group of experiments, the effect was observed with praseodymium, magnesium, and silver stearates. The cumulative yields should, of course, be identical. Three possible causes of the anomalies are (1) radiation damage effects in the stearate, (2) use of improper growth and decay genetics in the calculation of results, (3) iodine emanation, and (4) incomplete emanation of xenon after irradiation and admission of air.

Radiation damage is not a likely cause of the anomalous observations because it is known that short-lived rare gases emanate well at the total radiation dose delivered to the stearates in these experiments. Such an effect was ruled out by performing two experiments at 0.1 the reactor power level and, consequently, 0.1 the radiation damage rate of all the other experiments. The lower dose rate produced no noticeable effect on the results.

An experiment was performed to see if an appreciable fraction of the ^{133}Xe^m or ^{133}Xe^g is formed faster than expected as a result of a significant fraction of ^{133}I^m ($t_{1/2}=9$ sec) (Ref. 14) decaying to one or both of the xenon isomers. Tellurium was radiochemically purified from the fission products of ^{235}U by standard techniques involving reduction with SO_2 and $Fe(OH)_3$ scavenges. The pure sample was counted on a Ge(Li) detector. The observed decay and growth for 55.4-min ^{133}Te^m, 12.45-min ^{133}Te, and 20.3-h ^{133}I were in good agreement with that predicted using our current values for branching ratios, independent yields, and half-lives for the six-membered chain (^{133}Sb, ^{133}Te^m, ^{133}Te^g, ^{133}I, ^{133}Xe^m, and ^{133}Xe^g). No further account was taken of the existence of the 9-sec isomer of ^{133}I^m in this work. Analysis of the 81-keV peak of ^{133}Xe was complicated by several other photopeaks at or near 81 keV, and no conclusions can be made concerning agreement between experimental and predicted growth of ^{133}Xe isomers and decay of ^{133}I. The present evidence seems to indicate that unknown factors in the growth and decay genetics of the mass-133 chain have not been responsible for the anomalies that we have observed.

It is known that some iodine emanates from stearates, most likely as HI. Denschlag *et al.*[15] have determined that the iodine is not in organic forms such as CH_3I. We had determined that the fraction of iodine getting out of the irradiation container in our experiments was no more than about 0.4% because amounts larger than this were never found in the iodine traps and none was found in the xenon traps. After finding that larger quantities of iodine emanate and absorb on rubber stoppers (see below), we performed a series of experiments to check absorption of iodine on the materials we use. An emanation container with a large evacuated space was used, and various materials were suspended in this space. A uranium foil covered by magnesium stearate was placed in the bottom of the container to be irradiated. The inside of the container was also lined with paper so that the number of fissions could be determined by measuring the activities of ^{91}Sr and ^{140}Ba from the decay of ^{91}Kr and ^{140}Xe. Depending on conditions, 2—18 % of the ^{133}I or ^{135}I emanated. Such iodine had great affinity for rubber stoppers, moderate affinity for grease and paper, and low affinity for teflon, silicone-coated rubber, polyethylene, aluminum, and quartz wool. Only a few percent of the volatile iodine could be removed with the Xe.

A series of four experiments was conducted, in which only one xenon milk of each rabbit was made at times varying from 0.1 to 1 d. One of the purposes of these ex-

periments was to see whether, in the absence of any introduced air, xenon emanates quantitatively from the rabbit independently of the behavior of iodine precursors. The target foil in each case was ^{235}U, and the fission fragments were caught in magnesium stearate. The fission yields of the kryptons and xenons from the four experiments were the same and there is good agreement of the ratios of the fission yields with those given by Rider.[16]

In addition, we investigated the behavior of volatile iodine (^{133}I and ^{135}I) in these same four experiments. The amount of volatile iodine absorbed in the charcoal iodine trap varied from 2% to 4% of the total iodine present, as in other experiments. We also removed the rubber stoppers, sectioned them into quarters, and counted them. In all cases, only the inner quarter ($\cong 3$ mm) contained any ^{133}I and ^{135}I, which indicates that the volatile iodine does not diffuse deeply into the rubber. The amount of iodine on the stoppers increased from 2% to 19% as the milk time increased from 0.1 to 1 d. However, it appears that if air is not admitted into the rabbit after irradiation, the xenon daughter from any ^{133}I or ^{135}I in the rabbit—either in the stearate, in volatile form, or absorbed on a rubber stopper— emanates and can be quantitatively removed for measurement.

In a group of four experiments to determine the chemical separation factor for the second separation, the average factor was 0.842 with a population standard deviation of 0.026 for ^{133}Xe and ^{135}Xe. This factor was used in the chemical separation matrix C_2 to be described.

We hypothesize that the almost constant anomalous results obtained from second rare-gas milks came from chemical changes induced in the irradiated stearates when a small amount of air is introduced during the first milk. The oxygen in the air may react at sites in the stearate and prevent emanation of approximately 16% of the xenon that results from future decay of iodine.

The xenon samples were usually counted in Ge(Li) well counters because high efficiency was needed to give adequate counting rates. In a few experiments they were counted with coaxial Ge(Li) detectors. To determine the efficiencies of the well counters for the gamma rays under consideration, a comparison of count rates for the same samples was made using the well counters and Ge(Li) coaxial counters that had been calibrated with International Atomic Energy Agency standard reference sources. In every experiment, the same counting arrangement was used for the xenon from the first and second separations so that fractional independent yields could be determined independently of counting efficiency.

The particular gamma rays under consideration were $^{133}Xe^m$, 233 keV; $^{133}Xe^g$, 80 keV; $^{135}Xe^m$, 527 keV; and $^{135}Xe^g$, 250 keV. Early counting data for the 250-keV gamma ray from $^{135}Xe^g$ were not used because of interference from the gamma rays of ^{138}Xe. The intensities of the photopeaks were determined by the Los Alamos version of the BRUTAL code.[17] For selected examples the intensities were also determined with the GAMMANAL code.[18] In each case there was agreement within the errors provided by the codes.

Photopeak intensities at separation time for the 527-keV gamma ray of $^{135}Xe^m$ were obtained by the appropriate version of the Los Alamos PACKAGE (Ref. 19) least squares program. This version of PACKAGE determines the coefficients of a sum of exponentials. Counting rates corrected for dead time of the analyzer were used. Errors for individual intensities provided by BRUTAL were used. Analyzer dead times for intensities other than that of the 527-keV gamma ray from $^{135}Xe^m$ were negligible. The coefficients of the exponentials in the appropriate decay and growth equations for intensities other than the 527-keV gamma ray were determined by the SKITZO least squares program. SKITZO differs significantly from PACKAGE only in that SKITZO takes account of decay during counting. The errors that were input to SKITZO were the larger of 1% or the error provided by BRUTAL. (The use of these coefficients will be described later.) The 80-keV photopeak of $^{133}Xe^g$ from the first separation in each experiment shows growth resulting from the decay of $^{133}Xe^m$.

D. Radioactivity measurements

Because measurement of the independent yield of $^{135}Xe^m$ involves measurement of the 527-keV gamma ray of $^{135}Xe^m$ in the presence of orders of magnitude greater amounts of radiation from ^{138}Xe and its daughter ^{138}Cs, and because the half-life of ^{138}Xe is similar to that of $^{135}Xe^m$, it was necessary to determine whether there was any contribution from ^{138}Xe in the 527-keV region. Accordingly, a sample of radioactive Xe and Kr was separated from freshly irradiated uranyl stearate. The sample was then mass separated to obtain a sample of ^{138}Xe free from $^{135}Xe^m$. The ^{138}Xe and daughter activities were counted with a Ge(Li) detector in the same way that $^{135}Xe^m$ is normally counted. No peak in the 527-keV region was located by either the BRUTAL or SAMPO (Ref. 20) programs, nor was any distinct peak visible. There was a small excess of activity above the continuum in the 525—530-keV region, which decayed with a 15—20-min half-life. However, this excess may have been caused by variations in the continuum and is treated only as an upper limit to a possible real contribution. The intensity of this apparent activity was related to the 435-keV gamma ray of ^{138}Xe to give the following limit for the relative intensity of a contribution from ^{138}Xe to the 527-keV photopeak:

$$\left[\frac{\text{527-keV intensity}}{\text{435-keV intensity}}\right]_{^{138}Xe} \leq 0.008 .$$

In the experiments involving measurement of the independent yield of $^{135}Xe^m$ from either thermal-neutron or Godiva-IV-neutron fission of ^{235}U, the maximum contribution to the 527-keV photopeak region from ^{138}Xe is 5% of the total intensity observed for the 527-keV photopeak. The uncertainties used in our data analysis cover such an uncertainty.

For the experiments involving measurement of the independent yield of $^{135}Xe^m$ from Godiva-IV-neutron-induced fission of ^{238}U, attempts to observe the 527-keV gamma ray were as difficult as in the case of ^{138}Xe. There was an activity that decayed with the proper half-life and

that was three to four times as intense relative to the 435-keV gamma ray of ^{138}Xe as were those from the pure ^{138}Xe sample. However, we do not feel confident that we really observed any 527-keV photopeak in the ^{238}U fission experiments, and the activity was treated as an upper limit for ^{135}Xe^m activity without correction for contribution from ^{138}Xe.

The length of irradiation varied from a few milliseconds for Godiva-IV bursts up to about 10 min for some 14.8-MeV irradions. Thermal irradiations lasted from 0.5 to 1 min. The first xenon separation always occurred in less than 5 min (usually 2—3 min) after irradiation. The second xenon separation always occurred after sufficient time for substantial decay of xenon precursors; it was usually about a day after the irradiation. All times were measured to about 0.01 min. However, the uncertainty in the xenon separation times was either 0.25, 0.5, or 0.75 min, depending on whether the separation took 1, 2, or 3 min, respectively.

E. Method of calculation

The method by which the desired quantities (fractional independent yields, isomer ratios, etc.) and their errors were calculated is described in this section. A necessary part of the calculaton uses a subroutine based on Deming's[21] general least squares calculation. The subroutine is written so that the moment matrix of the errors in the data need not be diagonal. It is convenient to distinguish between several types of quantities. The parameters (the quantities to be determined) are denoted by the symbol A and include fractional independent yields, isomer ratios, etc. There are two categories of data denoted by symbols X and Z. Category X consists of counting efficiencies and counting rates or linear combinations of counting rates. Category Z includes X and also such values as half-lives, branching ratios, separation times, etc. The X's and Z's are not considered to be essentially different; it is convenient to treat them differently because of the method used to solve the differential equations of radioactive decay and growth. The A, X, and Z are column vectors. Subscripts are appended to indicate specific elements of the vectors. A similar notation is used for matrices, with the row index occurring first.

Error propagation is done by calculating the moment matrix M_A of the errors of the parameters A from the moment matrix M_Z of the errors in the data Z. The relation[22] between these moment matrices is

$$M_A = BM_Z B^T , \tag{1}$$

where

$$B_{ij} = \frac{\partial A_i}{\partial Z_j} , \tag{2}$$

and B^T is the transpose of B. The part of the matrix B due to X is provided by the Deming least squares subroutine. The rest of B is evaluated by incrementing each of the other items of data Z one at a time.

The calculation was carried out in three ways using different combinations of data from the same experiments.

(1) In the "two-separation" method S, the photopeak intensities in the same counting arrangement were compared for two Xe samples; one separated as soon as possible after irradiation and the other after significant decay of precursors has occurred. Detector efficiencies are not required because only a ratio of the photopeak intensities in the two samples is needed in the calculation. However, this method is sensitive to the values used for the iodine branching ratios and to the chemical separation factor for Xe. The fractional independent yields of each of the isomers was calculated and from these the isomer ratios were obtained.

(2) The "efficiency" method E uses primarily the photopeak intensities from the Xe sample separated immediately after irradiation. The appropriate photopeak efficiencies, conversion coefficients, etc., were used in the calculation of the ratio of the independently formed Xe isomers. The fractional independent yields themselves cannot be calculated unless information concerning the number of fissions in the sample is included in the calculation. This method is not as sensitive as method S to the branching ratios and is not dependent on the completeness of the recovery of Xe from the stearate. There is a small interaction with the results from method S because decay and growth corrections from method S are used.

(3) Method ES is a combination of methods E and S. It is used because the results from methods E and S are not independent and cannot be properly averaged. The parameters from methods E and S are used as initial approximations for method ES. Method ES is regarded as the most nearly correct method; methods E and S were used to check for internal consistency of the results. In one experiment, the data for method S were not available and the isomer ratio from method E was used for both ^{133}Xe and ^{135}Xe.

The following indexing is used for the $A=133$ chain: ^{133}Sb, 1; ^{133}Te^m, 2; ^{133}Te^g, 3; ^{133}I, 4; ^{133}Xe^m, 5; and ^{133}Xe^g, 6. For the $A=135$ chain, the indexing is ^{135}Te, 3; ^{135}I, 4; ^{135}Xe^m, 5; and ^{135}Xe^g, 6. The quantities corresponding to ^{133}Sb and ^{133}Te^m, whose indices would be 1 and 2, respectively, are missing for the 135 chain.

During irradiation, species i is produced at a rate $r_i f(t)$, where $f(t)$ is proportional to the fissioning rate and r_i is proportional to the independent yield of species i. The r_i's are arranged into a column vector r. The number of atoms $N_i(t_1)$ of species i at the end of irradiation at time t_1 is an element of the column vector $N(t_1)$; $N(t_1)$ is related to r by a matrix $S(t_1)$:

$$N(t_1) = S(t_1) r . \tag{3}$$

The value of $S(t_1)$ comes from the solution, described in the Appendix, of the differential equations of decay and growth during irradiation.

Decay and growth after irradiation is represented by matrices $R(t_j - t_i)$ such that

$$N(t_j) = R(t_j - t_i) N(t_i) . \tag{4}$$

These matrices again come from the solution of the differential equations.

Chemical separations are represented by matrices with nonzero entries only along the main diagonal

$$C=\text{diag}(C_1,\ldots,C_n)\ ,$$

where C_i is the fraction of species i going into the portion of the fission products of interest. If the chemical separation that separates Xe from its precursors were complete, it would be represented by the matrix

$$C_1=\text{diag}(0,0,0,1,1)$$

for the Xe portion and by the matrix

$$C_2=\text{diag}(1,1,1,1,0,0)$$

for the other portion. These equations identify the matrices C_1 and C_2 for the subsequent discussion where the separations are not assumed to be complete.

There are two Xe separations, one at time t_2 as soon as possible after the irradiation, and another at time t_3 about a day later. The Xe from the first separation is represented at the time of separation by the matrix product

$$N(t_2)=C_1R(t_2-t_1)S(t_1)r=Dr\ . \tag{5}$$

The Xe from the second separation at time t_3 is represented by

$$N(t_3)=C_1R(t_3-t_2)C_2R(t_2-t_1)S(t_1)r=Er\ . \tag{6}$$

The second equations of (5) and (6) define matrices D and E. Equations (5) and (6) give

$$\begin{aligned} N_5(t_2)&=\sum_{j=1}^{6}D_{5j}r_j\ ,\\ N_6(t_2)&=\sum_{j=1}^{6}D_{6j}r_j\ ,\\ N_5(t_3)&=\sum_{j=1}^{6}E_{5j}r_j\ , \end{aligned} \tag{7}$$

and

$$N_6(t_3)=\sum_{j=1}^{6}E_{6j}r_j\ .$$

1. Mass 133

For the $A=133$ chain, Eqs. (7) are related to the data as follows: $N_5(t_2)$ and $N_5(t_3)$ are proportional to the intensity of the 233-keV gamma ray of $^{133}Xe^m$ at t_2 and t_3, respectively. These intensities are called X_1 and X_2, respectively. For methods S and ES,

$$F_1=X_1N_5(t_3)-X_2N_5(t_2)=0 \tag{8}$$

is an equation of condition for Deming's least squares calculation. For method E, X_1 is converted into atoms Y_1, and

$$F_1=Y_1-N_5(t_2) \tag{9}$$

leads to an equation of condition for Deming's least squares calculation in a way that is explained later. Here, $N_6(t_2)$ is proportional to X_3, which is defined as the sum of the coefficients of the 5.25- and 2.19-d exponentials at T_2. These were obtained from the SKITZO (Ref. 19) least squares treatment of the counting data for the 80-keV gamma ray from the ground state of ^{133}Xe. The moment matrix of the two coefficients, provided by SKITZO, is taken into account through Eq. (1) in calculating the standard deviation of all such sums of coefficients of exponentials. For method E, X_3 is converted into atoms Y_2 (Ref. 23), and

$$F_2=Y_2-N_6(t_2) \tag{10}$$

leads to an equation of condition for Deming's least squares treatment.

$$N_6(t_3)-\lambda_5N_5(t_3)/(\lambda_6-\lambda_5)$$

is proportional to the coefficient of the 5.25-d exponential. This coefficient calculated at t_3 is called X_4 and was also obtained from the SKITZO treatment of the counting data for the 80-keV gamma ray from the ground state of ^{133}Xe. For methods S and ES,

$$F_2=X_3[N_6(t_3)-\lambda_5N_5(t_3)/(\lambda_6-\lambda_5)]-X_4N_6(t_2)=0 \tag{11}$$

is an equation of condition.

2. Mass 135

For the $A=135$ chain, Eqs. (7) are related to the data as follows: $N_5(t_2)$ and $N_5(t_3)$ are proportional to the intensities of the 527-keV gamma ray of $^{135}Xe^m$ at t_2 and t_3, respectively, as determined graphically. These intensities are called X_1 and X_2, respectively. For methods S and ES,

$$F_1=X_1N_5(t_3)-X_2N_5(t_2)=0 \tag{12}$$

is an equation of condition. For method E, X_1 is converted into atoms Y_1, and

$$F_1=Y_1-N_5(t_2)=0 \tag{13}$$

leads to an equation of condition.

$$N_6(t_2)-\lambda_5N_5(t_2)/(\lambda_6-\lambda_5)$$

is proportional to the coefficients of the 9.104-h exponential at t_2 obtained from the SKITZO treatment of the counting rates of the 250-keV gamma ray from $^{135}Xe^g$. For method E, this coefficient, called X_3, is converted to atoms Y_2, and

$$F_2=Y_2-N_6(t_2)+\lambda_5N_5(t_2)/(\lambda_6-\lambda_5)=0 \tag{14}$$

leads to another equation of condition. Similarly,

$$N_6(t_3)-\lambda_5N_5(t_3)/(\lambda_6-\lambda_5)$$

is proportional to the coefficient of the 9.104-h exponential at t_3, which is called X_4. Then for methods S and ES,

$$F_2=X_3[N_6(t_3)-\lambda_5N_5(t_3)/(\lambda_6-\lambda_5)]-X_4[N_6(t_2)-\lambda_5N_5(t_2)/(\lambda_6-\lambda_5)]=0 \tag{15}$$

is an equation of condition.

In counting the 250-keV gamma ray from $^{135}Xe^g$ from the separation at t_2, the early data are not used because

the 250-keV photopeak is masked by the much more intense 259- and 243-keV gamma rays of ^{138}Xe. In counting the 250-keV gamma ray from the separation at t_3, no growth caused by the decay of ^{135}Xe^m is observed. Thus, for both samples only the coefficient of the 9.104-h exponential is available, and it must be interpreted as above.

3. *Mass 133 and Mass 135*

For methods S and ES, the sums in (7) representing N's in Eqs. (8), (11), (12), and (15) were used in the form

$$\sum_{i=1}^{6} d_i r_i = A_1(d_1 s_1 + d_2 s_2 + d_3 d s_3) + r_4 d_4 + A_2 d_5 + A_3 d_6 \,, \tag{16}$$

where d_i is E_{5i}, E_{6i}, D_{5i}, D_{6i}, or such linear combinations of them as occur in Eqs. (11), (14), and (15). In Eq. (16),

$$s_i = r_i/(r_1+r_2+r_3) \,,$$

where $i=1,2,3$; r_4 is the fractional independent yield of iodine; and the A's are parameters evaluated by the least squares method. Values A_2 and A_3 are the fractional independent yields of the metastable and ground states of Xe, respectively. The values s_1, s_2, s_3, and r_4 were fixed in each least squares calculation for evaluating the B_{ij}'s in Eq. (2); they were incremented one at a time and the least squares calculation repeated. For the $A=135$ chain, $s_1=s_2=0$ and $s_3=1$. For both chains and for methods S and ES,

$$F_3 = A_1(s_1+s_2+s_3)+r_4+A_2+A_3-1=0$$

is an equation of condition. This equation is necessary for normalization.

For method E, the r's from method S were used as follows. For any one of the sums (16) we have the identity

$$d_5 r_5 + d_6 r_6 = \sum_{i=1}^{6} d_i r_i \left[1 - \frac{\sum_{i=1}^{4} d_i r_i}{\sum_{i=1}^{6} d_i r_i} \right] . \tag{17}$$

In this identity, $\sum_{i=1}^{6} d_i r_i$ is replaced by the appropriate Y. See, for example, Eq. (9). Thus, the equations of condition take the form

$$d_5 A_1 + d_6 A_2 = Y \left[1 - \frac{\sum_{i=1}^{4} d_i r_i}{\sum_{i=1}^{6} d_i r_i} \right] , \tag{18}$$

where A_1 and A_2 are parameters to be evaluated by the least squares procedure. They are the rates at which the metastable and ground state isomers of Xe, respectively, are formed directly by fission during the irradiation. The term

$$1 - \frac{\sum_{i=1}^{4} d_i r_i}{\sum_{i=1}^{6} d_i r_i}$$

is evaluated from the results of method S, and thus, as

TABLE III. Half-lives and branching ratios used in calculations.

Isotope	Half-life	Daughter	Branching ratio
^{133}Sb	2.5±0.2 min[a]	^{133}Te^m	0.165±0.021[b]
		^{133}Te^g	0.835±0.021[b]
^{133}Te^m	55.4±0.4 min[c]	^{133}Te^g	0.17±0.02[d]
		^{133}I	0.83±0.02[d]
^{133}Te^g	12.45±0.28 min[e]	^{133}I	1
^{133}I	20.60±0.25 h[f]	^{133}Xe^m	0.029±0.001[g]
		^{133}Xe^g	0.971±0.001[g]
^{133}Xe^m	2.19±0.05 d[h]	^{133}Xe^g	1
^{133}Xe^g	5.25±0.02 d[h]		
^{135}Te	17.5±0.08 sec[i]	^{135}I	1
^{135}I	6.64±0.06 h[j]	^{135}Xe^m	0.147±0.007[k]
		^{135}Xe^g	0.853±0.007[k]
^{135}Xe^m	15.48±0.28 min[l]	^{135}Xe^g	1
^{135}Xe^g	9.104±0.020 h[h]		

[a]References 24—28.
[b]References 48 and 49.
[c]Reference 29.
[d]Reference 48.
[e]Reference 30.
[f]References 31—35.
[g]References 14 and 47.
[h]Reference 36.
[i]References 37—39.
[j]References 40—44.
[k]Reference 50.
[l]References 43, and 45—47.

TABLE IV. Fractional independent and fractional cumulative yields used in the calculations.

	Fractional cumulative yield of ^{133}Sb	Fractional independent yield ^{133}Te	^{133}I	^{135}I
Thermal-neutron-induced fission				
^{233}U	0.11 ±0.04[a]	0.68 ±0.11[a]	0.146±0.012[b]	0.606±0.024[c]
^{235}U	0.326±0.04[d]	0.60 ±0.05[e]	0.025±0.003[f]	0.46 ±0.02[g]
^{239}Pu	0.174±0.011[h]	0.618±0.033[h]	0.151±0.028[c]	0.608±0.017[c]
^{242}Am^{m}	0.30 ±0.09[i]	0.60 ±0.1[i]	0.10 ±0.06[i]	0.57 ±0.10[i]
Godiva-IV-neutron-induced fission				
^{235}U	0.31 ±0.06[i]	0.29 ±0.1[i]	0.048±0.036[i]	0.53 ±0.12[i]
^{238}U	0.7 ±0.1[i]	0.29 ±0.1[i]	0.000285±0.000285[i]	0.131±0.060[i]
^{239}Pu				0.60 ±0.14[j]
14.7-MeV-neutron-induced fission				
^{235}U	0.054±0.050[i]	0.60 ±0.15[i]	0.32 ±0.10[i]	
^{238}U	0.38 ±0.15[j]	0.58 ±0.15[j]	0.05 ±0.05[i]	
^{239}Pu	0.022±0.022[i]	0.39 ±0.13[i]	0.53 ±0.15[i]	

[a]References 51 and 52.
[b]References 51 and 53.
[c]Reference 53.
[d]Reference 55.
[e]References 52 and 54.
[f]Reference 56.
[g]Reference 37.
[h]Reference 52.
[i]Estimated from systematics by the methods of Ref. 57.
[j]Average of the methods of Refs. 57 and 58.

mentioned earlier, the two methods are not completely independent.

The following errors were used for both chains: (1) length of irradiation: 0.01 min, except for the Godiva-IV irradiations, where the value 4.17×10^{-8} min was used; (2) time of the first Xe separation: 0.5 min for thermal-neutron-induced fission of ^{239}Pu and 0.25 min for all others; (3) time of second Xe separation: 0.5 min for thermal-neutron-induced fission of ^{239}Pu and 0.25 min for all others; and (4) fractional independent yields of Sb (133 chain only) and Te isomers: 0.5 the estimated fractional independent yield.

The following items with their errors were used: (1) fraction of Sb, Te, and I isomers remaining in the irradiation containers when Xe was separated: 0.99±0.01; (2) fraction of Xe isomers remaining in the stearate when Xe was separated: 0.03±0.02; and (3) fraction of Xe isomers getting into the sample to be counted when Xe was separated: 0.97±0.01 for the first separation and 0.842±0.026 for the second separation.

The half-lives and branching ratios used in the calculations are given in Table III. The references from which the values were taken are also listed (Refs. 24—50). Where more than one reference is given, the error given in Table III is the standard deviation of the population of values in the references. The correlation coefficient of -1 was used to calculate the covariance in M_z of Eq. (1) for the two branching ratios for a single isotope.

Fractional independent yields and fractional cumulative yields used in the calculations are given in Table IV, in addition to the works from which they were taken (Refs. 37 and 51—58). The isomer ratio of ^{133}Te was taken to be 2.95±0.31 for all fissioning systems.

All quantities entering the calculations, whether they are our data, literature values, or estimates, have an assigned error and all errors were propagated by Eq. (1) as described above. Equation (1) is correct if increments in the parameters are linearly related to increments in the data.

Duplicate experiments are not independent and strictly should not be averaged because the same genetic information is used in all of them; nevertheless, we did average them as though they were independent.

In averaging n measurements, each measurement was given a weight equal to $\sigma_{\text{ext}}^2/\sigma^2$, where σ is the error of the measurement and σ_{ext}^2 (Ref. 21) is a constant (usually 1) for each average. In some cases, the sum of the squares of the weighted deviations was greater than one. In these cases, σ_{ext}^2 was adjusted to make the sum of squares equal to $n-1$. This increased the resulting error of the average. All such cases are identified below in the following section.

III. RESULTS AND DISCUSSION

A. Experimental results

The results of our measurements and other, previously published measurements are given in Tables V–IX for neutron-induced fission of ^{233}U, ^{235}U, ^{238}U, ^{239}Pu, and ^{242}Am^m. Although the sum and ratio of the fractional independent yields of the isomers can be calculated from the individual fractional independent yields, the same is not true of their errors because the errors of the individual yields are correlated. The sum and ratio and their errors are, therefore, given separately.

For thermal-neutron-induced fission of ^{233}U, our fractional independent yield of ^{135}Xe agrees with that of Hawkings, Edwards, and Olmstead[43] and nearly agrees with that of Okazaki, Walker, and Bigham.[59] For thermal-neutron-induced fission of ^{235}U, our fractional independent yield of ^{135}Xe nearly agrees with that of Blachot,[60] but our isomer ratios and fractional independent yields for ^{133}Xe and ^{135}Xe do not agree with measurements by Hsu, Lin, Yang, and Yu.[61] For 14.8-MeV neutron-induced fission of ^{235}U, we either agree or nearly agree with isomer ratios and fractional independent yields of ^{133}Xe and ^{135}Xe measured by Alexander.[62] For 14.8-MeV neutron-induced fission of ^{238}U, our fractional independent yields agree with those of Alexander[62] for both ^{133}Xe and ^{135}Xe, and our isomer ratio agrees with that of Alexander for ^{135}Xe. For 14.8-MeV neutron-induced fission of ^{239}Pu, our isomer ratios for ^{133}Xe and ^{135}Xe and our fractional independent yield of ^{135}Xe agree with those of Alexander.[62] However, our fractional independent yield for ^{133}Xe does not agree with that of Alexander.

Our measured fractional independent yields (the sum of the fractional independent yields of both isomers) have been compared[63] with Wahl's Z_p (Ref. 64) and A_p' (Ref. 65) models for charge distribution for thermal-neutron-induced fission of ^{233}U, ^{235}U, and ^{239}Pu. Sufficient data to make such comparisons for other fissioning systems have not been assembled. The Z_p model deals with the dispersion of fractional independent yields with Z at constant A, whereas the A_p' model deals with the dispersion of independent yields with A at constant Z. The A_p' model represents the data better than the Z_p model near the 50-proton shell. Values of calculated yields from both models as well as our experimental yields are given in Table X.

Spinrad and Wu[66] have found that

$$\delta u = |\ln(Y_c/Y_e)|\ ,$$

where Y_c and Y_e are calculated (from a Z_p model) and experimental fractional independent yields, respectively, can be represented (with much scatter) by a linear function of $(Z-Z_p)^2$. This linear equation, with rounded off parameters, was used to estimate values of δu for ^{133}Xe and ^{135}Xe from which expected model uncertainties were estimated. A model uncertainty is an estimate of how

TABLE V. The ^{133}Xe and ^{135}Xe fractional independent yields and isomer ratios for thermal-neutron-induced fission of ^{233}U.[a,b]

^{133}Xe^m	0.006 48±0.000 69[c]
^{133}Xe^g	0.002 69±0.000 17
^{133}Xe^m+^{133}Xe^g	0.009 20±0.000 73[c]
^{133}Xe^m/^{133}Xe^g	2.42±0.23[c]
^{135}Xe^m	0.128±0.017
^{135}Xe^g	0.0994±0.0092
^{135}Xe^m+^{135}Xe^g	0.232±0.014
	0.218±0.004[d]
	0.182±0.16[e]
^{135}Xe^m/^{135}Xe^g	1.24±0.20

[a]Average of two experiments.
[b]Fissionable material A in Table I.
[c]Error adjusted as explained in the text.
[d]Reference 43.
[e]Reference 59.

TABLE VI. The ^{133}Xe and ^{135}Xe fractional independent yields and isomer ratios for neutron-induced fission of ^{235}U.[a]

	Thermal neutrons	Godiva-IV neutrons	14.8-MeV neutrons
^{133}Xe^m	0.000 266±0.000 017[b]	0.000 674±0.000 033	0.0259±0.0012
^{133}Xe^g	0.000 085±0.000 017	0.000 164±0.000 039	0.005 10±0.000 55
^{133}Xe^m+^{133}Xe^g	0.000 354±0.000 019	0.000 837±0.000 052	0.0310±0.0014
	0.07±0.03[c]		0.022±0.007[d]
^{133}Xe^m/^{133}Xe^g	2.85±0.50	3.92±0.92	4.90±0.57
	0.35±0.19[c]		>2[d]
^{135}Xe^m	0.0256±0.0031[b]	0.0298±0.0017	0.1599±0.0070
^{135}Xe^g	0.0143±0.0018	0.0175±0.0042[b]	0.083±0.011
^{135}Xe^m+^{135}Xe^g	0.0395±0.0041[b]	0.0475±0.0039[b]	0.2431±0.0075
	0.050±0.005[c]		0.26±0.01[d]
	0.11±0.02[c]		
^{135}Xe^m/^{135}Xe^g	1.77±0.29	1.48±0.34[b]	1.92±0.32
			1.2±0.2[e]

[a]Fissionable materials B, C, D, and E in Table I.
[b]Error adjusted as explained in the text.
[c]Reference 60.
[d]Reference 61.
[e]Reference 62.

TABLE VII. The ^{133}Xe and ^{135}Xe fractional independent yields and isomer ratios for neutron-induced fission of ^{238}U.[a]

	Godiva-IV neutrons	14.8-MeV neutrons
$^{133}Xe^m$	<0.0015	$0.002\,38\pm0.000\,10$
$^{133}Xe^g$	<0.00025	$0.000\,47\pm0.000\,14$
$^{133}Xe^g+^{133}Xe^m$	<0.0017	$0.002\,86\pm0.000\,14$
		0.003 ± 0.0013[b]
$^{133}Xe^m/^{133}Xe^g$		4.9 ± 1.5
$^{135}Xe^m$	<0.0066	0.0287 ± 0.0041[c]
$^{135}Xe^g$	<0.0069	0.0188 ± 0.0023
$^{135}Xe^m+^{135}Xe^g$	$0.006\,00\pm0.000\,71$	0.0497 ± 0.0032[c]
		0.056 ± 0.037[b]
$^{135}Xe^m/^{135}Xe^g$		1.39 ± 0.25[c]
		1.4 ± 0.7[b]

[a]Fissionable material *F* in Table I.
[b]Reference 62.
[c]Error adjusted as explained in the text.

TABLE VIII. The ^{133}Xe and ^{135}Xe fractional independent yields and isomer ratios for neutron-induced fission of ^{239}Pu.[a]

	Thermal neutrons	Godiva-IV neutrons	14.8-MeV neutrons
$^{133}Xe^m$	$0.004\,66\pm0.000\,26$[b]		0.0575 ± 0.0081[b]
$^{133}Xe^g$	$0.001\,30\pm0.000\,11$		0.0170 ± 0.0012
$^{133}Xe^m+^{133}Xe^g$	$0.005\,97\pm0.000\,25$		0.0751 ± 0.0085[b]
			0.120 ± 0.001[c]
$^{133}Xe^m/^{133}Xe^g$	3.44 ± 0.26[d]		3.39 ± 0.40[b]
			2.6 ± 0.8[c]
$^{135}Xe^m$	0.0867 ± 0.0046[b]		0.317 ± 0.021
$^{135}Xe^g$	0.0598 ± 0.0063		0.117 ± 0.025
$^{135}Xe^m+^{135}Xe^g$	0.1467 ± 0.0079[b]		0.4337 ± 0.0097
			0.46 ± 0.03[c]
$^{135}Xe^m/^{135}Xe^g$	1.41 ± 0.16[d]	2.03 ± 0.38[e]	2.69 ± 0.74
			3.5 ± 1.6[c]

[a]Fissionable materials *G* and *H* in Table II.
[b]Error adjusted as explained in the text.
[c]Reference 62.
[d]Average of three determinations; two by method *ES* and one by method *E*.
[e]Average of three determinations by method *E*.

TABLE IX. The ^{133}Xe and ^{135}Xe fractional independent yields and isomer ratios for thermal-neutron-induced fission of $^{242}Am^m$.

$^{133}Xe^m$	$0.004\,71\pm0.000\,49$[a]
$^{133}Xe^g$	$0.001\,64\pm0.000\,13$
$^{133}Xe^m+^{133}Xe^g$	$0.006\,40\pm0.000\,41$[a]
$^{133}Xe^m/^{133}Xe^g$	2.80 ± 0.44[a]
$^{135}Xe^m$	0.0869 ± 0.0054
$^{135}Xe^g$	0.0500 ± 0.0075
$^{135}Xe^m+^{135}Xe^g$	0.1390 ± 0.0047
$^{135}Xe^m/^{135}Xe^g$	1.73 ± 0.35

[a]Error adjusted as explained in the text.

TABLE X. Comparison of measured fractional independent yields of ^{133}Xe and ^{35}Xe from thermal-neutron-induced fission with charge distribution systematics.

	Measured fractional independent yield	Calculated yield	Agreement factor
	^{133}Xe		
^{233}U	0.009 20±0.000 73		
Z_p model		0.006 08	0.8
A_p' model		0.004 68	0.4
^{235}U	0.000 354±0.000 019		
Z_p model		0.000 226	0.6
A_p' model		0.000 148	0.3
^{239}Pu	0.005 97±0.000 25		
Z_p model		0.002 89	1.4
A_p' model		0.001 73	0.9
^{242}Am^m			
Nethaway's model[a]	0.006 40±0.000 41	0.003 14	1.3
	^{135}Xe		
^{233}U	0.232±0.014		
Z_p model		0.196	0.6
A_p' model		0.158	0.7
^{235}U	0.0395±0.0041		
Z_p model		0.0203	0.7
A_p' model		0.0337	0.4
^{239}Pu	0.1467±0.0079		
Z_p model		0.116	0.8
A_p' model		0.079	1.1
^{242}Am^m			
Nethaway's model[a]	0.1390±0.0047	0.132	0.16

[a]Calculated by the method of Ref. 58.

well the model can be expected to represent a true fractional independent yield. A similar expression for the A_p' model expresses δu as a linear function of $(A-A_p')^2$. The parameters were adjusted to take account of the greater width of the distribution in A. The ratio of $|Y_c-Y_e|$ to the square root of the sum of the squares of the model uncertainty and the experimental error is called the agreement factor.[63] It is a measure of the degree of agreement between calculated and experimental fractional independent yields for a particular isotope. Agreement factors are given in Table X. Most of the agreement factors for Wahl's A_p' and Z_p models in Table X are less than 1, and this represents better than expected agreement.

Sufficient data have been assembled by Wolfsberg[57] to permit comparison with an older adaptation of the Z_p model for all our fissioning systems except thermal-neutron-induced fission of ^{242}Am^m. All our measurements are within the limits given by Wolfsberg.

Another adaptation of the Z_p model by Nethaway[58] deals with systematic trends with changes of the fissioning nucleus and its excitation energy. Results for this model are given in Table X for thermal neutron induced fission of ^{242}Am^m. The agreement factors for ^{133}Xe and ^{135}Xe are greater than and less than 1, respectively.

Isomer ratios for ^{131}Te and ^{133}Te have been measured. Their metastable and ground states have the same spin and parity ($\frac{11}{2}^-$ and $\frac{3}{2}^+$, respectively) as the metastable and ground states of ^{133}Xe and ^{135}Xe. They are, therefore, included in the following discussion. We have chosen the following values of isomer ratios for ^{131}Te: thermal-neutron-induced fission of ^{233}U, 1.88 (Ref. 52); thermal-neutron-induced fission of ^{235}U, 1.91 (Ref 52); thermal-neutron-induced fission of ^{239}Pu, 2.12 (Ref. 52); 33-MeV α-particle-induced fission of ^{232}Th, 3.3 (Ref. 2); 18-MeV deuteron-induced fission of ^{232}Th, 2.7 (Ref. 2); 33-MeV α-particle-induced fission of ^{238}U, 5.0 (Ref. 2); and 18-MeV deuteron-induced fission of ^{238}U, 3.3 (Ref. 2). For ^{133}Te we have chosen the following isomer ratios: thermal-neutron-induced fission of ^{233}U, 1.32 (Ref. 52); thermal-neutron-induced fission of ^{235}U, 1.31 (Ref. 52); thermal-neutron-induced fission of ^{239}Pu, 1.61 (Ref. 52); 33-MeV α-particle-induced fission of ^{232}Th, 2.8 (Ref. 2); 18-MeV deuteron-induced fission of ^{232}Th, 1.7 (Ref. 2); 33-MeV α-particle induced fission of ^{238}U, 3.1 (Ref. 2); and 18-MeV deuteron-induced fission of ^{238}U, 1.8 (Ref. 2). Isomer ratios for ^{133}Xe and ^{135}Xe are from this work. Also some isomer ratios for ^{133}Te as a function of the kinetic energy E_k of the fragment[28] have been measured for thermal-neutron-induced fission of ^{235}U and are discussed here. They are 0.87 for $E_k=83.4$ MeV and 4.11 for $E_k=68.7$ MeV.

A least squares line was fit to our measured ^{133}Xe and ^{135}Xe isomer ratios as a function of neutron energy for neutron-induced fission of ^{235}U (Fig. 1) and as a functior

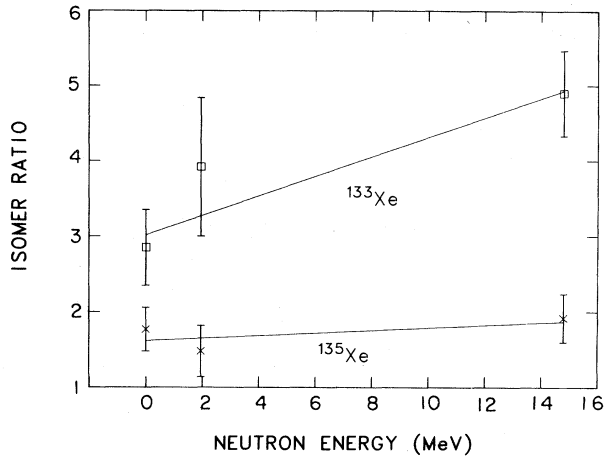

FIG. 1. Dependence of isomer ratios on the energy of the neutron inducing fission.

of the J value of the target nucleus for thermal-neutron-induced fission (Fig. 2). Confidence intervals for the slopes with a 95% confidence coefficient were derived from the variance of the slopes. This was done to include a slope of either $+\infty$ or $-\infty$ in an attempt to exclude zero because we are trying to show a dependence on either neutron energy or angular momentum. The assertion that the isomer ratio of ^{135}Xe does not depend on either the J value of the target or on the neutron energy is consistent with our results at the 5% confidence level. On the other hand, such an assertion about ^{133}Xe is not consistent with our results at the 5% confidence level. We take this as experimental evidence that isomer ratios depend on the fission process; i.e., they are not completely determined by the nature of the fission product. These results are also experimental evidence that the isomer ratio for ^{135}Xe depends less on the fission process than the isomer ratio for ^{133}Xe does. (This point will be discussed later. The dependence of isomer ratios on the nature of the fission product will be discussed at length.)

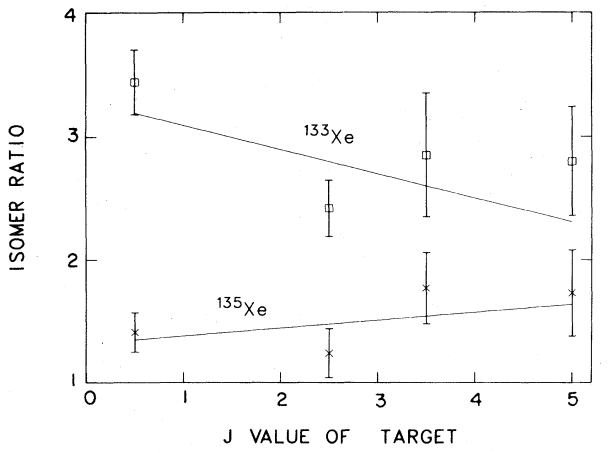

FIG. 2. Dependence of isomer ratios on the J value of the target.

Further evidence that isomer ratios depend on the fission process comes from the range of values measured as neutron energy and target vary. Our measured isomer ratios for ^{135}Xe vary from 1.24 ± 0.20 for thermal-neutron-induced fission of ^{233}U to 2.69 ± 0.79 for 14.8-MeV neutron-induced fission of ^{239}Pu. Our measured isomer ratios for ^{133}Xe include a value 2.43 ± 0.23 for thermal-neutron-induced fission of ^{233}U and a value 4.94 ± 0.58 for 14.8-MeV neutron-induced fission of ^{235}U. The difference between the isomer ratios of ^{133}Xe and ^{135}Xe also indicates that isomer ratios depend on the fission products. This dependence is reflected in nuclear level densities as a function of energy, angular momentum, and parity.

B. Interpretation of isomer ratios

We have calculated isomer ratios and various other values using a statistical model. We used calculated level densities for the four isotopes under consideration as a function of excitation energy E, total angular momentum quantum number J, and parity π. These calculations were done by the combinatorial method of Ref. 67, with single-particle states[68] for a spherical Woods-Saxon potential.[69] The simple method used in Ref. 67 to take account of pairing effects did not significantly improve the agreement between calculated and measured level densities; it was not used in the calculations described here. In this model there is no obvious way to separate energy into intrinsic and rotational parts. The use of combinatorially calculated level densities is the major difference between our calculations and similar calculations. For the following discussion, the $2J+1$ degenerate states with angular momentum quantum number J count as $2J+1$ states and one level. The space-fixed direction with respect to which the projection of the angular momentum m is defined is the direction of motion of the fission fragment. (The reason for this definition will be discussed later.) States with energy only up to the neutron separation energies are included; it is presumed that more energetic fission products will emit a neutron. The neutron separation energies are ^{131}Te, 5.924 MeV; ^{133}Te, 5.795 MeV; ^{133}Xe, 6.448 MeV; and ^{135}Xe, 6.451 MeV. All the energy bins for a given fission product were equal, and all were near 0.164 MeV. The states and levels depend only on the single-particle states of the fission product; they are taken to be the points of a probability space where the probabilities are determined by the fission process. The number of levels in the energy bin with midpoint E, angular momentum quantum number J, and parity π is denoted by $\rho(E,J,\pi)$. We will try to derive some information about these probabilities from measured isomer ratios. Some assumptions must be made about a type of functional dependence of the probabilities on E and J. All levels from the combinatorial calculation in and below the energy bin of the observed $\frac{11}{2}^-$ isomer were replaced by those of the observed $\frac{11}{2}^-$ isomer and $\frac{3}{2}^+$ ground state.

The four fission products under consideration have very different combinatorially calculated state densities. This fact is related to the single-particle state structure near the Fermi surface; its effect on calculated isomer ratios is dis-

cussed later. The total number of states with energy below 4.8 MeV (a completely arbitrary energy) are given in Table XI. The ratio of the number of states for the telluriums, 64, and for the xenons, 39, are principally the result of the extra 2 neutrons in ^{133}Te and ^{135}Xe and their occupancy of the 18 neutron single-particle states in the $1h\frac{11}{2}^-$, $3s\frac{1}{2}^+$, and $2d\frac{3}{2}^+$ levels. The single-particle states with energies below (above) the 18 neutron single-particle states are usually (seldom) occupied, at least for energies considered here, and do not make a large contribution to the state and level densities. The binomial coefficients[70] are $\binom{18}{15}$ for ^{131}Te and $\binom{18}{17}$ for ^{133}Te. The ratio of these coefficients is 45, which should be compared with the ratios of 64 and 39 in Table XI. The comparison is not exact because other single-particle states are involved sometimes and because the $1h\frac{11}{2}^-$, $3s\frac{1}{2}^+$, and $2d\frac{3}{2}^+$ levels do not have exactly the same energy for the four nuclei. The other two ratios in Table XI are for common neutron numbers of 79 and 81; the origin of the differing numbers of states is the extra two protons in ^{133}Xe and ^{135}Xe and their occupancy of the 26 states of the $1g\frac{7}{2}^+$, $2d\frac{5}{2}^+$, and $1h\frac{11}{2}^-$ proton single-particle levels. The ratio of the binomial coefficients $\binom{26}{4}$ to $\binom{26}{2}$ is 46 and should be compared with the ratios 27 and 45 in Table XI. Various results of our statistical model calculations, other than state densities, depend on the single-particle state structure near the Fermi surface, but not in the simple way that state densities do.

We chose to let the probabilities of different states depend on E, J, and m but not on π. For this purpose an exponential dependence for E and J is used; i.e., the probability of a state is taken to be proportional to $\exp(-\beta E-\lambda J)$, where β and λ depend on the fission process, which in this context includes everything that occurs before the fission product is formed at an energy below the neutron separation energy. The units of β are MeV^{-1}, and λ has no units. The dependence of the probabilities on m values is discussed later. The exponential factor is the result of maximizing the information theory entropy[71] $H=-\sum p_i \log p_i$ (the sum is over all states under consideration and p_i is the probability of state i), subject to the constraints that E and J have specified average values. This is the justification for using the exponential rather than some other function for the dependence of the probabilities on E and J. The quantities β and λ are Lagrange multipliers for the constrained maximum, and if there is thermal equilibrium (which we do not suggest), it is appropriate to call $1/\beta$ the temperature. (The Boltzmann constant is taken to be 1.) The quantity $J(J+1)$ could be used instead of J. Taking $\beta=\lambda=0$ assigns equal probabilities to all states and produces the maximum value of H that is possible for a given set of states. Taking $\beta=\lambda=0$ also produces values for a single isomer ratio, average energy, etc., that do not depend on the fission process but depend only on the fission product. The β and λ are the only adjustable parameters in our treatment, and as will be seen, β is unimportant in relating isomer ratios to average angular momentum.

TABLE XI. Number of states for ^{131}Te, ^{133}Te, ^{133}Xe, and ^{135}Xe with energy below 4.8 MeV.

	$N=79$	$N=81$	Ratio
$Z=52$	850 243(^{131}Te)	13 208(^{133}Te)	64
$Z=54$	23 295 002(^{133}Xe)	598 814(^{135}Xe)	39
Ratio	27	45	

It is generally believed[72,73] that the angular momentum of fission fragments before neutron emission tends to be perpendicular to the direction of motion; this means that m is approximately zero because m is the projection of the angular momentum in the direction of motion. The m value should still be near zero for the fission products, i.e., after the emission of prompt neutrons. We take the initial probabilities to be zero for $m>0.5$ and equal for $m=\pm 0.5$. This amounts to assuming that two states for each level are initially occupied. Thus, we have an initial ensemble of nuclei such that the number in energy bin E with angular momentum number J and parity π is given by

$$g_0(E,J,\pi)=2\rho(E,J,\pi)\exp(-\beta E-\lambda J) .$$

The values $\langle E\rangle$, $\langle J\rangle$, and $\langle J(J+1)\rangle$ are averages over the initial ensemble and do not depend on further calculations, which will be described later. The distribution of the initial ensemble of nuclei as a function of E and J for ^{133}Te for various values of β and λ are shown in Figs. 3–6. The values plotted are

$$\sum_{\pi} g_0(E,J,\pi) \Big/ \sum_{E,J,\pi} g_0(E,J,\pi) .$$

The values plotted in Fig. 3, where β and λ are both zero, are proportional to $\rho(E,J,+)+\rho(E,J,-)$.

Many previous treatments[73–75] of isomer ratios (but not all[76]) have not considered any explicit dependence of the probabilities on energy. The formula

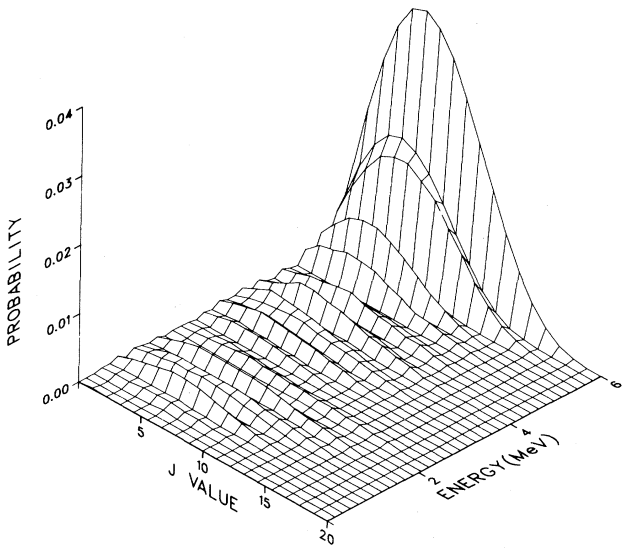

FIG. 3. Probability distribution as a function of energy and J value for ^{133}Te with $\beta=0$ and $\lambda=0$. The calculated isomer ratio is 2.12.

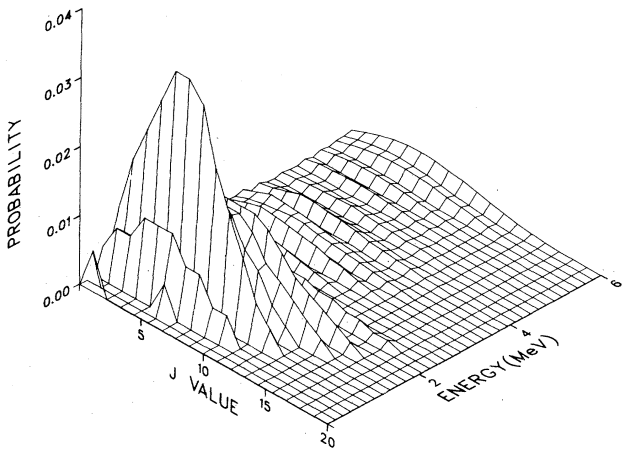

FIG. 4. Probability distribution as a function of energy and J value for ^{133}Te with $\beta=1$ and $\lambda=0$. The calculated isomer ratio is 2.03.

$$P(J) \propto (2J+1)\exp[-J(J+1)/B^2] , \quad (19)$$

or some minor variant, is usually used in these treatments.

For each gamma-ray transition, we use the subscripts i and f to denote the initial and final states of the nucleus, respectively. The angular momentum quantum number of the gamma ray and its projection on the direction of motion of the fission fragment are denoted by L and M, respectively.

We assume, as has been implicitly assumed in previous treatments, that the system behaves as a Markov chain after the initial formation of Te or Xe with excitation energy below the neutron separation energy. This is the same as assuming that once the nucleus is known to be in an initial state, the conditional probability of a transition to each final state does not depend on the previous history of the nucleus. Relative (i.e., not yet normalized) conditional probabilities are taken to be proportional to the

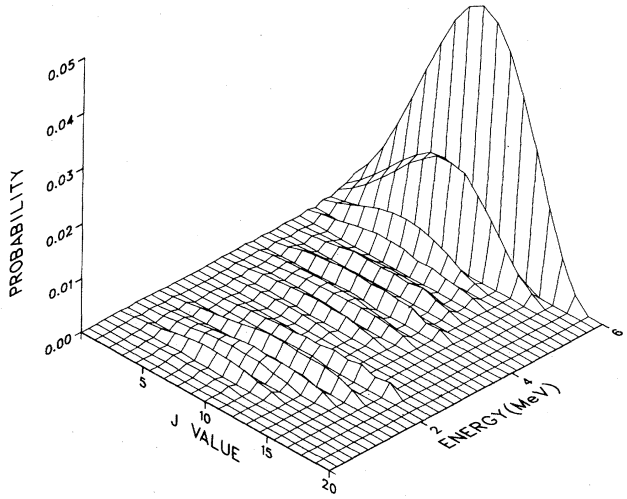

FIG. 5. Probability distribution as a function of energy and J value for ^{133}Te with $\beta=0$ and $\lambda=-0.24$. The calculated isomer ratio is 6.99.

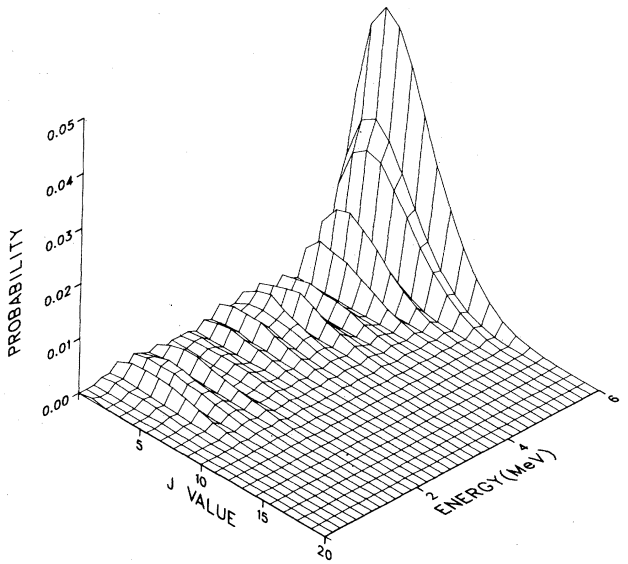

FIG. 6. Probability distribution as a function of energy and J value for ^{133}Te with $\beta=0$ and $\lambda=0.24$. The calculated isomer ratio is 0.83.

values for the transition probability T_{sp} (with $A=133$) given by Moszkowski;[77] Moszkowski's statistical factors S are modified as discussed below. The energy E_γ of the gamma ray is E_i-E_f. The values T_{sp} were $2.6\times10^{15}\ E_\gamma^3$ for $E1$ transitions, $2.9\times10^{13}\ E_\gamma^3$ for $M1$ transitions, $5.0\times10^{10}\ E_\gamma^5$ for $E2$ transitions, and $2.9\times10^{9}\ E_\gamma^5$ for $M2$ transitions.

Moszkowski's statistical factors are not appropriate for our calculations because they involve averaging some integrals over all initial m values, with equal probabilities, whereas we have assumed zero initial probability for $|m|>0.5$. The individual terms over which Moszkowski averages depend on M, m_i, and m_f but are zero unless $M=m_i-m_f$. Thus, there are not more than the smaller of $2L+1$ or $2J_f+1$ nonzero terms for each final state. We use the symbol R for the smaller of $2L+1$ or $2J_f+1$. To avoid keeping track of m values throughout the calculation, we assume that there are R nonzero statistical factors for each final state and that these have the value 1. This amounts to taking the number of final states equal to $R\rho(E_f,J_f,\rho_f)$. Because we are not keeping track of m values, it is possible that $m_f>J_f$ or $m_i>J_i$ could occur and that we are assuming a value of 1 for terms that should be zero. To check the effect of this, we also did all our calculations with $R=2$. Isomer ratios were a few tenths of 1% lower than with the R described above.

At step n of the calculation (not step n of the gamma-ray cascade), there are $g_n(E_i,J_i,\pi_i)$ initial states and zero or more final states; E_f ranges through each value such that $E_f<E_i$. Relative conditional probabilities for transitions from initial state i to final state f are calculated as described above and normalized to give conditional probabilities p_{if}. Because only dipole and quadrupole transitions are being considered $p_{if}=0$ for $L>2$. The values of $g_{n+1}(E_f,J_f,\rho_f)$ are given by

$$g_{n+1}(E_f,J_f,\pi_f)=g_n(E_f,J_f,\pi_f)$$
$$+p_{if}g_n(E_i,J_i,\pi_i)R\rho(E_f,J_f,\pi_f)\ .$$

At step n in this calculation, i is fixed and f ranges over all possible final states. The calculation starts with g_0 and ends when the only remaining E_f is the energy of the lowest energy bin.

During the calculation we keep track of the energy of each gamma ray. This permits the calculation of the average energy per gamma ray and the average number of gamma rays. We do not assume *a priori* any particular number of gamma rays. We also keep track of the number of gamma rays with $L>1$.

At the end of the calculation, there are some members of the ensemble left in fairly low energy bins with $J>\frac{11}{2}$ that cannot decay to either the $\frac{3}{2}^+$ ground state or the $\frac{11}{2}^-$ isomer by gamma rays with $L\leq 2$. These nuclei are said to be trapped and are attributed to the $\frac{11}{2}^-$ isomer. The number of nuclei in the $\frac{11}{2}^-$ state is then divided by the number in the $\frac{3}{2}^+$ ground state to give the calculated isomer ratio.

Calculations were done for the four fission products under consideration in the rectangle $0\leq\beta\leq 1$, $-0.24\leq\lambda\leq 0.24$ to determine the dependence of various quantities on β, λ, and the fission product. This range of values is more than enough to cover the range of measured isomer ratios. As β changes from 0 to 1, there is a large change in the distribution of the initial ensemble of nuclei (as can be seen in Figs. 3 and 4), whereas $\langle J\rangle$, $\langle J(J+1)\rangle^{1/2}$, the isomer ratio, and the fraction of trapped nuclei change by less than 11% for the four nuclei considered here. Thus, virtually nothing can be learned about the initial energy distribution by measuring isomer ratios. The fraction of gamma rays with $L>1$ changes by as much as 23% with this change in β. As λ changes from -0.24 to $+0.24$, there is not much change in the distribution of the initial ensemble of nuclei (as may be seen in Figs. 5 and 6), but there is considerable change in $\langle J\rangle$, $\langle J(J+1)\rangle^{1/2}$, the isomer ratio, and the fraction of trapped states. The average of the initial energies $\langle E\rangle$ varies from 34% to 64% as β changes from 0 to 1; it increases as the number of states with energy ≤ 4.8 MeV increases. The energy per gamma ray depends more on the fission product than on either β or λ; it increases as λ increases, decreases as β increases, and increases as $\langle E\rangle$ increases. The number of gamma rays per fission product does not depend very much on either β or λ but does depend on the isotope; it increases with the number of states with energy <4.8 MeV.

In one set of calculations for ^{135}Xe, 23 observed levels[14] were substituted for 14 601 calculated levels in $\rho(E,J,\pi)$ for all energies up to the energy of the highest observed level. Observed levels without angular momentum and parity assignments were omitted. Isomer ratios were 8—13 % lower than when calculated levels were used for all energies. Calculated levels were used for all of the results presented here because the levels excited in decay scheme studies are not necessarily the same as those that occur in a gamma-ray cascade in a fission product.

Calculated isomer ratios for ^{133}Xe depend more on λ than calculated isomer ratios for ^{135}Xe do. This is in agreement with our earlier observation that measured isomer ratios for ^{133}Xe depend more on the fission process than measured isomer ratios for ^{135}Xe do.

Measurements by Pleasanton *et al.*[78] of average gamma-ray energy, average number of gamma rays, and average energy of gamma rays as a function of mass number cannot be directly compared with our calculations because the measurements are not for the four isotopes under consideration, but are averages over several atomic numbers for a given mass. It appears, however, that our results for these quantities are only consistent with measurements of Pleasanton *et al.* for values of $\beta>0$. We have accordingly chosen to use a value of $\beta=1$. Such results are given in Table XII. Negative values of λ (a preference for higher J values) are required for some isomer ratios for ^{131}Te, ^{133}Te, and ^{133}Xe but not for ^{135}Xe.

Because both $\langle J\rangle$ and the isomer ratio are nearly independent of β and depend strongly on λ, there is a fairly good functional relation of each on λ and, therefore, a fairly good functional relation, different for each isotope, between $\langle J\rangle$ and the isomer ratio. Curves showing the relation between $\langle J\rangle$ and the isomer ratio for ^{131}Te, ^{133}Te, ^{133}Xe, and ^{135}Xe are shown in Fig. 7. A similar curve from formula (19), calculated by the method given by Madland and England[74] for all cases where the J value and parity of the isomer and ground states are $\frac{11}{2}^-$ and $\frac{3}{2}^+$, respectively, is also given in Fig. 7. Our curves for ^{131}Te and ^{135}Xe are nearly coincident over the range of isomer ratios for which both were calculated, and the ratio of the calculated number of states with energy less than 4.8 MeV is 1.4. The curves for ^{133}Te and ^{133}Xe do not coincide, and the ratio of the calculated number of states with energy less than 4.8 MeV is about 1700. These results suggest that the relation between $\langle J\rangle$ and the isomer ratio depends strongly on the number of states with energy less than some specified value, which in turn, as was shown above, depends mainly on the single-particle configuration near the Fermi surface.

The average J value, number of gamma rays per fission,

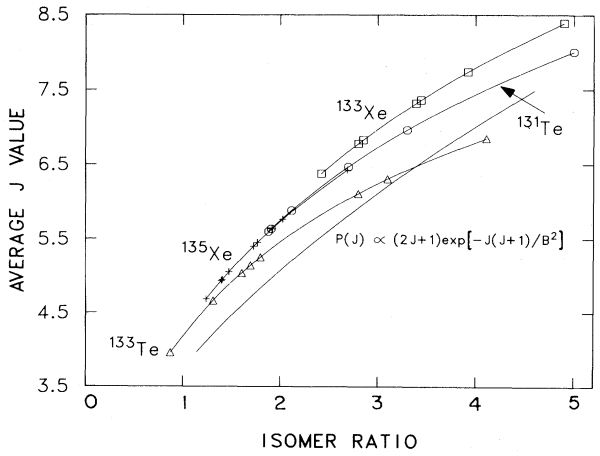

FIG. 7. Average J values as a function of calculated isomer ratios for $\beta=1$. The curves are nearly the same for other reasonable values of β.

TABLE XII. Results of the statistical calculations.

Reaction	Isomer ratio	λ	Average energy (MeV)	Average J value	Square root of average $J(J+1)$	Fraction of γ rays with $L>1$	Fraction of trapped states	Energy per γ ray	Number of γ rays per fission product
$^{233}U(n_{th},F)^{131}Te$	1.88[a]	0.0940	2.51	5.60	6.91	0.125	0.083	0.72	3.25
$^{235}U(n_{th},F)^{131}Te$	1.91[a]	0.0906	2.51	5.63	6.95	0.126	0.085	0.72	3.25
$^{239}Pu(n_{th},F)^{131}Te$	2.12[a]	0.0687	2.51	5.88	7.21	0.134	0.098	0.72	3.27
$^{232}Th(d_{18},F)^{131}Te$	2.7[b]	0.0205	2.53	6.47	7.81	0.154	0.133	0.71	3.29
$^{232}Th(\alpha_{33},F)^{131}Te$	3.3[b]	−0.0172	2.54	6.96	8.32	0.171	0.166	0.71	3.31
$^{238}U(\alpha_{33},F)^{131}Te$	5.0[b]	−0.0887	2.57	8.01	9.36	0.208	0.245	0.71	3.35
$^{235}U(n_{th},F)^{133}Te$	0.87[c]	0.2093	1.75	3.95	5.07	0.110	0.055	0.70	2.20
$^{235}U(n_{th},F)^{133}Te$	1.31[a]	0.1039	1.76	4.66	5.80	0.131	0.096	0.68	2.25
$^{233}U(n_{th},F)^{133}Te$	1.32[a]	0.1020	1.76	4.67	5.82	0.131	0.097	0.68	2.25
$^{239}Pu(n_{th},F)^{133}Te$	1.61[a]	0.0538	1.76	5.04	6.19	0.143	0.123	0.66	2.27
$^{232}Th(d_{18},F)^{133}Te$	1.7[b]	0.0409	1.77	5.14	6.29	0.146	0.131	0.66	2.28
$^{238}U(d_{18},F)^{133}Te$	1.8[b]	0.0276	1.77	5.25	6.40	0.150	0.139	0.66	2.28
$^{232}Th(\alpha_{33},F)^{133}Te$	2.8[b]	−0.0709	1.78	6.11	7.25	0.184	0.215	0.64	2.31
$^{238}U(\alpha_{33},F)^{133}Te$	3.1[b]	−0.0923	1.79	6.30	7.44	0.192	0.234	0.64	2.32
$^{235}U(n_{th},F)^{133}Te$	4.11[d]	−0.1495	1.80	6.85	7.97	0.217	0.291	0.64	2.33
$^{233}U(n_{th},F)^{133}Xe$	2.42[e]	0.0908	3.23	6.37	7.83	0.118	0.251	0.76	4.05
$^{242}Am^{m}(n_{th},F)^{133}Xe$	2.80[e]	0.0635	3.24	6.78	8.25	0.126	0.286	0.75	4.06
$^{235}U(n_{th},F)^{133}Xe$	2.85[e]	0.0603	3.24	6.83	8.30	0.127	0.291	0.75	4.07
$^{239}Pu(n_{th},F)^{133}Xe$	3.39[e]	0.0298	3.26	7.32	8.81	0.138	0.334	0.75	4.09
$^{239}Pu(n_{14},F)^{133}Xe$	3.44[e]	0.0273	3.27	7.36	8.86	0.139	0.337	0.75	4.09
$^{235}U(n_{G},F)^{133}Xe$[f]	3.92[e]	0.0055	3.27	7.74	9.24	0.147	0.371	0.75	4.11
$^{235}U(n_{14.8},F)^{133}Xe$	4.90[e]	−0.0297	3.28	8.39	9.90	0.161	0.428	0.75	4.14
$^{238}U(n_{14.8},F)^{133}Xe$	4.9[e]	−0.0297	3.28	8.39	9.90	0.161	0.428	0.75	4.14
$^{233}U(n_{th},F)^{135}Xe$	1.24[e]	0.1867	2.32	4.68	5.94	0.110	0.120	0.71	2.81
$^{238}U(n_{14},F)^{135}Xe$	1.4[e]	0.1585	2.32	4.94	6.21	0.117	0.139	0.70	2.82
$^{239}Pu(n_{th},F)^{135}Xe$	1.41[e]	0.1568	2.32	4.95	6.23	0.117	0.141	0.70	2.82
$^{235}U(n_{G},F)^{135}Xe$[f]	1.48[e]	0.1458	2.32	5.06	6.34	0.120	0.149	0.70	2.82
$^{242}Am^{m}(n_{th},F)^{135}Xe$	1.73[e]	0.1113	2.33	5.40	6.70	0.129	0.177	0.69	2.83
$^{235}U(n_{th},F)^{135}Xe$	1.77[e]	0.1064	2.33	5.45	6.75	0.131	0.181	0.69	2.84
$^{235}U(n_{14.8},F)^{135}Xe$	1.92[e]	0.0892	2.33	5.63	6.94	0.136	0.197	0.68	2.85
$^{239}Pu(n_{G},F)^{135}Xe$[f]	2.03[e]	0.0775	2.33	5.76	7.07	0.139	0.209	0.68	2.85
$^{239}Pu(n_{14.8},F)^{135}Xe$	2.69[e]	0.0213	2.34	6.42	7.75	0.158	0.269	0.67	2.88

[a]Reference 52.
[b]Reference 2.
[c]Reference 28. The kinetic energy of the fission fragment was 83.4 MeV.
[d]Reference 28. The kinetic energy of the fission fragment was 68.7 MeV.
[e]This work.
[f]Subscript G indicates Godiva-IV neutrons.

fraction of trapped nuclei, fraction of gamma rays with $L>1$, and the isomer ratio decrease as λ increases. The average energy per gamma ray increases as λ increases.

Isomer ratios for ^{133}Te as a funcion of fragment kinetic energy (0.87 for 83.4 MeV and 4.11 for 68.7 MeV) will now be discussed. For this purpose, we calculated $\langle J\rangle$ for ^{134}Te as a function of β and λ for energies from 7.8 MeV (the neutron separation energy) up to 15 Mev. As noted above, for lower energies $\langle J\rangle$ depends strongly on λ and very little on β. Thus, it makes very little difference for the immediate purpose whether the ^{133}Te is formed directly or from ^{134}Te through neutron evaporation (which changes $\langle J\rangle$ very little). A value of about 6.9 for $\langle J\rangle$ is required to produce an isomer ratio of 4.11. This can be obtained with $\lambda=0$, so that no particular effect of fission dynamics on angular momentum need be invoked for this case. A value of 4 for $\langle J\rangle$ is required to produce an isomer ratio of 0.87, and this requires a value for λ of about 0.2, regardless of the value of β. Thus at higher kinetic energies, the fission dynamics must produce a tendency toward lower J values. This is consistent with higher kinetic energy fragments being nearly spherical, and therefore, having lower torques acting on them.

Our values of $\langle J(J+1)\rangle^{1/2}$ may be compared with values obtained by Wilhelmy *et al.*[73] for $\langle(J+0.5)^2\rangle^{1/2}$. Their values range from 6.15 to 10.05 in the mass region from $A=118$ to 140 for spontaneous fission of ^{252}Cf.

Hoffman[72] found that the fraction of quadrupole transitions for all fission products for thermal-neutron-induced fission of ^{233}U, ^{235}U, and ^{239}U is 0.15. This may be compared with our values for the fraction of gamma rays with $L>1$ in Table XII, which ranges from 0.110 up to 0.217.

ACKNOWLEDGMENTS

We wish to thank D. C. Hoffman and J. E. Sattizahn for support and encouragement. We also wish to thank A. C. Wahl for valuable discussions about charge distribution systematics and for performing the calculations that permitted a comparison of our measurements with systematics. We thank D. G. Madland for valuable discussions, D. R. Nethaway for help with the irradiations at Lawrence Livermore National Laboratory, and T. F. Wimmet and A. E. Evans for help with the irradiations at the Los Alamos Godiva and Crockroft Walton Facilities, respectively. This work was supported by the Defense Advanced Projects Agency, Order No. 1836.

APPENDIX: SOLUTION OF THE DIFFERENTIAL EQUATIONS

The differential equations were solved as follows to obtain the matrices S and R of (3)—(6).

The differential equations are

$$\begin{aligned}
\frac{dN_1(t)}{dt}&=A_{11}N_1(t)+r_1f(t)\ ,\\
\frac{dN_2(t)}{dt}&=A_{21}N_1(t)+A_{22}N_2(t)+r_2f(t)\ ,\\
&\vdots\\
\frac{dN_n}{dt}&=A_{n1}N_1(t)+\cdots+A_{nn}N_n(t)+r_nf(t)\ .
\end{aligned}\tag{A1}$$

$A_{ii}=-\lambda_i$ where λ_i is the decay constant. $A_{ji}=\lambda_iB_{ji}$ where B_{ji} is the fraction of species i that decays to species j. The indexing must be done so that $j\geq i$. The $r_if(t)$'s are rates of formation by means other than decay of precursors. The r_i's may be taken as proportional to independent yields. The differential Eqs. (A1) can be written in matrix form as

$$N'(t)=An(t)+rf(t)\ .\tag{A1'}$$

Coddington and Levinson[79] give the solution of (A1') as

$$N(t)=\exp[(t-\tau)A]N(\tau)+\int_\tau^t\exp[(t-s)A]rf(s)ds\ .\tag{A2}$$

$N(\tau)$ is a vector of initial or boundary conditions; i.e., the solution takes on the value $N(\tau)$ at the time $t=\tau$. The matrix $S(t_1)$ comes from the second term of (A2) and $R(t_i,t_j)$ comes from the first term.

Because A is a triangular matrix, its eigenvalues are the A_{ii}'s. It is known from linear algebra that if the A_{ii}'s are all different, then A is diagonalizable; i.e., a matrix P exists such that

$$A=P\,\mathrm{diag}(A_{11},\ldots,A_{nn})P^{-1}\ .$$

We deal only with the case where all the A_{ii}'s are different. The other case leads to terms like $te^{-\lambda_it}$, $t^2e^{-\lambda_it}$, etc., as explained by Coddington and Levinson.[79]

To obtain $S(t_1)$, take $\tau=0$, $N(\tau)=0$, and $t=t_i$ in (A2). Then

$$N(t_1)=\int_0^{t_1}\exp[(t_1-s)A]rf(s)ds\ .$$

Some matrix multiplications result in

$$N(t_1)=P\,\mathrm{diag}[F_1(t_1),\ldots,F_n(t_1)]P^{-1}r\ ,\tag{A3}$$

where

$$F_i(t_1)=r_i\int_0^{t_1}\exp[(t_1-s)A_{ii}]f(s)ds\ .\tag{A4}$$

The manipulations involve the relations

$$\exp[(t-s)A]=\exp[(t-s)PJP^{-1}]=P\exp[(t-s)J]P^{-1}=P\,\mathrm{diag}\{\exp[(t-s)A_{11}],\ldots,\exp[(t-s)A_{nn}]\}P^{-1}\ ,$$

where $J=P^{-1}AP=\mathrm{diag}(A_{11},\ldots,A_{nn})$. The relations follow from the definition[79]

$$\exp(B)=I+B+\frac{1}{2!}B^2+\frac{1}{3!}B^3+\cdots$$

of the exponential of a matrix B. The matrix $S(t_1)$ is $P\,\mathrm{diag}[F_1(t_1),\ldots,F_n(t_1)]P^{-1}$.

To obtain the matrices $R(t_j-t_i)$, put $f(s)=0$ and $N(\tau)=N(t_1)$ in Eq. (A2). Then

$$N(t_j)=\exp[(t_j-t_i)A]N(t_i) .$$

A somewhat abbreviated version of the manipulations mentioned above gives

$$N(t_j)=P\,\mathrm{diag}\{\exp[(t_j-t_i)A_{11}],\ldots,\exp[(t_j-t_i)A_{nn}]\}P^{-1}N(t_i) .$$

Thus $R(t_j-t_i)$ is given by

$$R(t_j-t_i)=P\,\mathrm{diag}\{\exp[(t_j-t_i)A_{11}],\ldots,\exp[(t_j-t_i)A_{nn}]\}P^{-1} .$$

Computer programs have been written to calculate P, P^{-1}, $S(t_i)$, and $R(t_j-t_i)$. The programs depend on matrix diagonalization, which replaces the commonly used process of assembling Bateman[80] solutions for all possible paths from each species to each of its descendants. The advantage is that attention need be paid only to the arrows in the decay scheme and not to all of the paths.

It should be noted that the structure of the decay scheme is at first embodied in matrix A and is transferred to matrix P in the solution. All of the time dependence is in the diagonal matrices $\mathrm{diag}[F_1(t_1),\ldots,F_n(t_1)]$ or $\mathrm{diag}\{\exp[(t_j-t_i)A_{11}],\ldots,\exp[(t_j-t_i)A_{nn}]\}$.

---

[1]A. C. Wahl, R. L. Ferguson, D. R. Nethaway, D. E. Troutner, and K. Wolfsberg, Phys. Rev. **126**, 1112 (1962).

[2]D. G. Sarantites, G. E. Gordon, and C. D. Coryell, Phys. Rev. **138**, B353 (1965).

[3]A. C. Wahl, J. Inorg. Nucl. Chem. **6**, 263 (1958).

[4]T. F. Wimett, R. H. White, and R. G. Wagner, in *Proceedings of the National Topical Meeting on Fast Burst Reactors, Albuquerque, New Mexico, 1969,* edited by R. L. Long and P. D. O'Brien (U. S. AEC, 1969), pp. 95–104.

[5]A. Turkevich and J. B. Niday, Phys. Rev. **84**, 52 (1951).

[6]G. P. Ford, Phys. Rev. **118**, 1261 (1960).

[7]H. B. Levy, H. G. Hicks, W. E. Nervik, P. C. Stevenson, J. B. Niday, and J. C. Anderson, Jr., Phys. Rev. **124**, 544 (1961).

[8]G. P. Ford and R. B. Leachman, Phys. Rev. **137**, B826 (1965).

[9]N. E. Ballou (private communication).

[10]R. W. Hoff, H. D. Wilson, R. W. Lougheed, M. S. Coops, J. E. Evans, and B. J. Qualheim, *155th American Chemical Society Meeting, San Francisco, 1968,* (Craftsman, Bladensburg, Maryland, 1968), Abstract 0-134.

[11]K. Wolfsberg and G. P. Ford, Phys. Rev. C **3**, 1333 (1971).

[12]K. Wolfsberg, G. P. Ford, and H. L. Smith, J. Nucl. Energy, Parts A and B **20**, 588 (1966).

[13]K. Wolfsberg, Phys. Rev. **137**, B929 (1965).

[14]*Table of Isotopes,* 7th ed., edited by C. M. Lederer and V. S. Shirley (Wiley, New York, 1978).

[15]H. O. Denschlag *et al.* (private communication).

[16]B. F. Rider, Vallecitos Nuclear Center Report NEDO-12154-3(c), 1981.

[17]R. Gunnink, H. B. Levy, and J. B. Niday, *153rd American Chemical Society Meeting, Miami Beach, 1967,* (Spaulding-Moss, Boston, 1967), Abstract N-6.

[18]R. Gunnink and J. B. Niday, Lawrence Livermore National Laboratory Report UCRL-51061, 1972.

[19]R. H. Moore and R. H. Zeigler, Los Alamos Scientific Laboratory Report LA-2367, 1959; P. McWilliams, Los Alamos Scientific Laboratory Report LA-2367, 1962.

[20]J. T. Routti and S. G. Prussin, Nucl. Instrum. Methods **72**, 125 (1969).

[21]W. E. Deming, *Statistical Adjustment of Data,* 1st ed. (Wiley, New York, 1938).

[22]Harald Cramér, *Mathematical Methods of Statistics* (Princeton University Press, Princeton, 1946), p. 298.

[23]The indexing is changed when X_3 is converted into Y_2 because X_2 is related to the second separation and is not used in method E.

[24]P. O. Strom, D. L. Love, A. E. Greendale, A. A. Deluchi, D. Sam, and N. E. Ballou, Phys. Rev. **144**, 984 (1966).

[25]G. Rudstam, E. Lund, L. Westgaard, and B. Grapengiesser, Proceedings of the International Conference on Properties of Nuclei Far from Region of Beta-Stability, Leysin, Switzerland, 1970, Vol. 1, p. 341, CERN Report CERN-70-30, 1970.

[26]H. N. Erten, J. Blachot, C. D. Coryell, and W. B. Walters (private communication), as quoted by E. A. Henry, Nucl. Data Sheets **11**, 495 (1974).

[27]M. M. Fowler, G. W. Goth, C. Lin, and A. C. Wahl, J. Inorg. Nucl. Chem. **36**, 1191 (1974).

[28]H. O. Denschlag, H. Braun, W. Faubel, G. Fischback, H. Meixler, G. Paffrath, W. Pörsch, M. Weis, H. Scharder, G. Siegert, J. Blachot, Z. B. Alfassi, H. N. Erten, T. Izak-Biran, T. Talmi, A. C. Wahl, and K. Wolfsberg in *Physics and Chemistry of Fission* (IAEA, Vienna, 1979), Vol. 2, p. 153.

[29]V. Berg, K. Franson, and C. E. Bemis, Ark. Fys. **37**, 213 (1968).

[30]S. G. Prussin and W. W. Meinke, Radiochim. Acta **4**, 79 (1965).

[31]S. Katcoff and W. Rubinson, Phys. Rev. **91**, 1458 (1953).

[32]A. C. Wahl, Phys. Rev. **99**, 730 (1955).

[33]G. Andersson, G. Rudstam, and G. Sorensen, Ark. Fys. **28**, 37 (1965).

[34]E. Eichler, J. W. Chase, N. R. Johnson, and G. D. O'Kelley, Phys. Rev. **146**, 899 (1966).

[35]S. A. Reynolds, J. F. Emery, and E. I. Wyatt, Nucl. Sci. Eng. **32**, 46 (1968).

[36]D. C. Hoffman, J. W. Barnes, B. J. Dropesky, F. O. Lawrence, G. M. Kelley, and M. A. Ott, J. Inorg. Nucl. Chem. **37**, 2336 (1975).

[37]H. O. Deschlag, J. Inorg. Nucl. Chem. **31**, 1873 (1969).

[38]S. Borg, G. B. Holm, and B. Rydberg, Nucl. Phys. **A212**, 197 (1973).

[39]H. D. Schüssler, H. Ahrens, H. Folger, H. Franz, W. Grimm, G. Herrmann, J. V. Kratz, and K. L. Kratz, in *Physics and Chemistry of Fission* (IAEA, Vienna, 1969).

[40]R. W. Dodson and R. D. Fowler, Phys. Rev. **57**, 966 (1940).

[41]L. E. Glendenin and R. P. Metcalf, in *Radiochemical Studies: The Fission Products,* edited by C. D. Corgell and N. Sugarman, National Nuclear Energy Series, Plutonium Project

Record, Div. IV (McGraw-Hill, New York, 1951), Vol. 9, p. 992.
[42]J. H. Landrum, A. L. Prindle, W. B. Walters, and R. A. Meyer, Bull. Am. Phys. Soc. **19**, 52 (1974).
[43]R. C. Hawkings, W. J. Edwards, and W. J. Olmstead, Can. J. Phys. **49**, 785 (1971).
[44]A. C. Pappas, Massachusetts Institute of Technology Report MIT-LNS-63 or U. S. Atomic Energy Agency Report AECU-2806, 1953; Nucl. Sci. Abs. **8**, 2273 (1954).
[45]T. Alvager, Ark. Fys. **17**, 521 (1960).
[46]K. Kotajima and H. Morinager, Nucl. Phys. **16**, 231 (1960).
[47]P. Alexander and J. P. Lau, Nucl. Phys. **A121**, 612 (1968).
[48]R. A. Meyer (private communication).
[49]L. Fujiwara, H. Imanishi, and T. Nishi, J. Inorg. Nucl. Chem. **36**, 1921 (1974).
[50]W. R. Daniels, G. P. Ford, D. C. Hoffman, and K. Wolfsberg, J. Inorg. Nucl. Chem. **36**, 201 (1974).
[51]L. A. Berge, Ph.D. thesis, University of Missouri, 1972.
[52]N. Imanishi, I. Fujiwara, and T. Nishi, Nucl. Phys. **A263**, 141 (1976).
[53]S. M. Qaim and H. O. Denschlag, J. Inorg. Nucl. Chem. **32**, 1767 (1970).
[54]A. A. Delucchi and A. E. Greendale, Phys. Rev. C **1**, 1491 (1970).
[55]R. W. Parsons and H. D. Sharma, J. Inorg. Nucl. Chem. **36**, 2392 (1974).
[56]A. C. Wahl, A. E. Norris, R. A. Rouse, and J. C. Williams, in *Physics and Chemistry of Fission* (IAEA, Vienna, 1969), p. 813.
[57]K. Wolfsberg, Los Alamos Scientific Laboratory Report LA-5553-MS, 1974.
[58]D. R. Nethaway, Lawrence Livermore Laboratory Report UCRL-51538, 1974.
[59]A. Okazaki, W. H. Walker, and C. B. Bigham, Can J. Phys. **49**, 498 (1971).
[60]J. Blachot (personal communication), as discussed in A. C. Wahl (unpublished).
[61]S. S. Hsu, J. T. Lin, C. M. Yang, and Y. W. Yu, Phys. Rev. C **24**, 523 (1981).
[62]P. Alexander, Nucl. Phys. **A198**, 228 (1972).
[63]A. C. Wahl (private communication).
[64]A. C. Wahl, J. Radioanal. Chem. **55**, 111 (1980).
[65]A. C. Wahl, in *New Directions in Physics and Chemistry,* edited by N. R. Metropolis and G.-C. Rota, (Academic, New York, to be published).
[66]B. I. Spinrad and C. H. Wu, Nucl. Sci. Eng. **66**, 421 (1978).
[67]G. P. Ford, Nucl. Sci. Eng. **66**, 334 (1978).
[68]G. P. Ford, D. C. Hoffman, and E. Rost, Los Alamos Scientific Laboratory Report LA-4329, 1970. Table I of this reference contains a typographical error; V_0 for rare-earth protons is $[48.5+50(N-Z)/A]$ MeV instead of the value given.
[69]R. D. Woods and B. S. Saxon, Phys. Rev. **95**, 577 (1954).
[70]The binomial coefficients $\binom{n}{v}$ are the number of combinations of n things taken v at a time. They are given by $\binom{n}{v}=n!/[(n-v)!v!]$.
[71]E. T. Jaynes, Phys. Rev. **106**, 620 (1957).
[72]M. M. Hoffman, Phys. Rev. **133**, B714 (1964).
[73]J. B. Wilhelmy, E. Cheifetz, R. C. Jared, S. G. Thomson, and H. R. Bowman, Phys. Rev. C **5**, 2041 (1972).
[74]D. G. Madland and T. R. England, Nucl. Sci. Eng. **64**, 859 (1977).
[75]J. R. Huizenga and R. V. Vandenbosch, Phys. Rev. **120**, 1305 (1960).
[76]J. P. Boquet, F. Schussler, E. Monnand, and K. Sistemich, *Physics and Chemistry of Fission* (IAEA, Vienna, 1979), Vol. 2, p. 179.
[77]S. A. Moszkowski, in *Alpha-, Beta-, and Gamma-Ray Spectroscopy,* edited by K. Seigbahn (North-Holland, Amsterdam, 1965), Chap. XV.
[78]F. Pleasanton, R. L. Ferguson, and H. W. Schmitt, Phys. Rev. C **6**, 1023 (1972).
[79]E. A. Coddington and N. Levinson, *Theory of Ordinary Differential Equations* (McGraw-Hill, New York, 1955).
[80]H. Bateman, Proc. Cambridge Philos. Soc. **15**, 423 (1910).